

Nernst effect and superconducting fluctuations in Zn-doped $\text{YBa}_2\text{Cu}_3\text{O}_{7-\delta}$

Z. A. Xu,* J. Q. Shen, and S. R. Zhao

Department of Physics, Zhejiang University, Hangzhou 310027, People's Republic of China

Y. J. Zhang and C. K. Ong

Department of Physics, National University of Singapore, Low Kent Ridge Road, Singapore 119260

(Received 4 April 2005; revised manuscript received 1 August 2005; published 28 October 2005)

We report the measurements of in-plane resistivity, Hall effect, and Nernst effect in Zn-doped $\text{YBa}_2\text{Cu}_3\text{O}_{7-\delta}$ epitaxial thin films grown by pulsed laser deposition technique. The pseudogap temperature T^* , determined from the temperature dependence of resistivity, does not change significantly with Zn doping. Meanwhile the onset temperature (T^v) of anomalous Nernst signal above T_{c0} , which is interpreted as evidence for vortex-like excitations, decreases sharply as the superconducting transition temperature T_{c0} does. A significant decrease in the maximum of vortex Nernst signal in mixed state is also observed, which is consistent with the scenario that Zn impurities cause a decrease in the superfluid density and therefore suppress the superconductivity. The phase diagram of T^* , T^v , and T_{c0} versus Zn content is presented and discussed.

DOI: [10.1103/PhysRevB.72.144527](https://doi.org/10.1103/PhysRevB.72.144527)

PACS number(s): 74.72.Bk, 74.20.-z, 74.62.Dh

I. INTRODUCTION

Effect of impurity doping is an important issue to discuss when considering the mechanism of high- T_c superconductivity. In the $\text{YBa}_2\text{Cu}_3\text{O}_{7-\delta}$ (YBCO) system, divalent Zn ions are believed to selectively substitute the planar Cu sites, which causes a sharp drop of T_c . The effects of a nonmagnetic impurity on the superconductivity have been theoretically predicted for a d -wave superconductivity.^{1,2} Experimental studies, including NMR,^{3,4} resistivity,⁵ surface impedance,⁶ electronic specific heat,⁷ optical spectra,^{8,9} neutron scattering,¹⁰ muon spin rotation,^{11,12} and Raman-scattering studies,¹³⁻¹⁶ have been performed to investigate the effect of Zn doping in YBCO system. These studies have suggested the pair-breaking effect and/or the decrease in the superfluid density due to Zn doping accounts for the radical suppression of superconductivity.

Recent Nernst effect measurements on high- T_c superconducting (HTS) cuprates have shown very surprising results.¹⁷⁻¹⁹ The Nernst effect is the appearance of a transverse electric field E_y in response to a temperature gradient $-\nabla T \parallel \hat{x}$, in the presence of a perpendicular magnetic $\mathbf{H} \parallel \hat{z}$ and under open circuit conditions. The Nernst effect is usually small in the normal state of metals where transport by quasiparticles is dominant. However, for a type-II superconductor (in the vortex-liquid state), a new set of excitations—vortices—are driven by temperature gradient $-\nabla T \parallel \hat{x}$. Vortices diffuse down the gradient with velocity $\mathbf{v} \parallel \hat{x}$. As each vortex core cross the line between a pair of transverse voltage electrodes, the 2π phase slip of the condensate phase leads to a Josephson \mathbf{E} field given by $\mathbf{E} = \mathbf{B} \times \mathbf{v}$, which is called vortex Nernst effect.

The experiments by Ong and collaborators¹⁷⁻¹⁹ have uncovered a large Nernst signal in the nonsuperconducting state of hole-doped cuprates, at temperatures well above the critical temperature T_c . The effect is particularly pronounced in underdoped samples, extending well into the “pseudogap” region of the cuprate phase diagram. The authors have interpreted this anomalous Nernst signal above T_c as evidence for

vortexlike excitations, and suggest that it is related to the pseudogap or some interaction between the pseudogap state and the superconducting state. This discovery has inspired a revisit to the theory of superconducting fluctuations in the cuprates. The conjecture that significant superconducting fluctuations in the pseudogap region give rise to the large Nernst signal is accord with the idea on the pseudogap proposed by Emery and Kivelson²⁰ that attributes its various anomalies to fluctuating superconductivity. Kontani suggests that the behaviors of Nernst signal below the pseudogap temperature (T^*) can be explained as the reflection of the enhancement of the d -wave superconducting fluctuations and antiferromagnetic (AF) fluctuations, without assuming thermally excited vortices.²¹ Ussishkin *et al.*²² calculate the contribution of Gaussian superconducting fluctuations to the transverse thermoelectric response above T_c and find that the Gaussian fluctuations are sufficient to explain the Nernst effect in the optimally doped and overdoped samples. Moreover the importance of the phase fluctuation of the complex order parameter ψ has been taken into account in theoretic models.^{20,23} In the work of Carlson *et al.*,²⁴ the fluctuations in the phase of the order parameter would dominate the Nernst signal up to a certain temperature above T_c .

The possibility that other exotic excitations in a strongly correlated state cause the anomalous Nernst effect is not excluded. For example, Weng and Muthukumar²⁵ suggest that in the description of spin-charge separation based on the phase string theory of the t - J model, thermally excited spinons destroy phase coherence, leading to a new phase characterized by the presence of free spinon vortices at temperatures $T_c < T < T_v$. The temperature scale T_v , at which holon condensation occurs marks the onset of the pairing amplitude and is related to the spin-pseudogap temperature T^* . The phase below T_v , called the spontaneous vortex phase, shows novel transport properties before phase coherence sets in at T_c , and the Nernst effect is regarded as an intrinsic characterization of such a phase.

In this paper, we report the measurements of resistivity, Hall effect, and Nernst effect on the Zn-doped $\text{YBa}_2\text{Cu}_3\text{O}_{7-\delta}$

epitaxial thin films. We find that Zn doping induces significant decrease of the vortex Nernst signal in mixed state, the onset temperature (T^v) of anomalous Nernst signal above T_{c0} , as well as the superconducting transition temperature (T_{c0}). Our results can be understood in the scenario that Zn doping leads to a decrease in superfluid density. The phase diagram of T^* , T^v , and T_{c0} versus Zn content is presented and discussed.

II. EXPERIMENTAL

The *c*-axis-oriented epitaxial $\text{YBa}_2(\text{Cu}_{1-x}\text{Zn}_x)_3\text{O}_{7-\delta}$ ($x=0, 0.005, 0.01, 0.02$) thin films were grown by pulsed laser deposition (PLD) method on LaAlO_3 substrates which were cut into a rectangle dimension of $10 \times 5 \text{ mm}^2$. The Zn content was determined by the composition of the targets which were prepared by standard solid state reaction. The temperature of the substrates was typically $720 \text{ }^\circ\text{C}$, and oxygen pressure was 25 Pa during the deposition. The thickness of the films was estimated to be about 200 nm according to the deposition time. To get optimal oxygen content, the samples were annealed at $500 \text{ }^\circ\text{C}$ for half an hour under 1 atm pure oxygen and δ was estimated to be less than 0.05 . X-ray diffraction shows that the films are *c*-axis oriented perpendicular to the substrate surface.

For electric resistivity and Hall effect measurements, six golden electrodes were deposited on each film. The in-plane resistivity $\rho(T)$ was measured by standard four-probe method. The Hall coefficient $R_H(T)$ was measured under a magnetic field of 5 T parallel to the *c* axis of the film. We define the (*x, y*) plane as the conducting *ab* plane of the film samples. In the setup of Nernst effect measurement, a temperature gradient of about 3 K/cm is applied along longitudinal direction (*x* direction), and the magnetic field H is applied along the *z* direction (perpendicular to the thin film surface). Thus the Nernst electric field is along the *y* direction, which was measured by Keithley Model 2182 Nanovoltmeter. The temperature gradient was measured by two small Cernox bare-chip thermometers (CX-1050-BR) which were attached to the two ends of the sample. A small heater is on the free end of the sample. All the measurements are based on a Quantum Design PPMS-9 system with the temperature drift less than 0.05% . The Nernst coefficient ν is defined as

$$\nu \equiv \frac{E_y}{-\nabla_x T B_z}. \quad (1)$$

We also define the Nernst signal as $e_y \equiv E_y / (-\nabla_x T)$. The Nernst signal was measured at positive and negative field polarities, and the difference of the two polarities was taken to remove any thermopower contribution. Since e_y is not linear with B as $T < T_{c0}$, the Nernst coefficient ν in the mixed state was calculated from the initial slope of e_y versus B_z .

III. RESULTS AND DISCUSSION

Figure 1 shows the temperature dependence of in-plane resistivity ρ for Zn-doped $\text{YBa}_2(\text{Cu}_{1-x}\text{Zn}_x)_3\text{O}_{7-\delta}$ ($x=0, 0.005, 0.01, 0.02$) thin films.

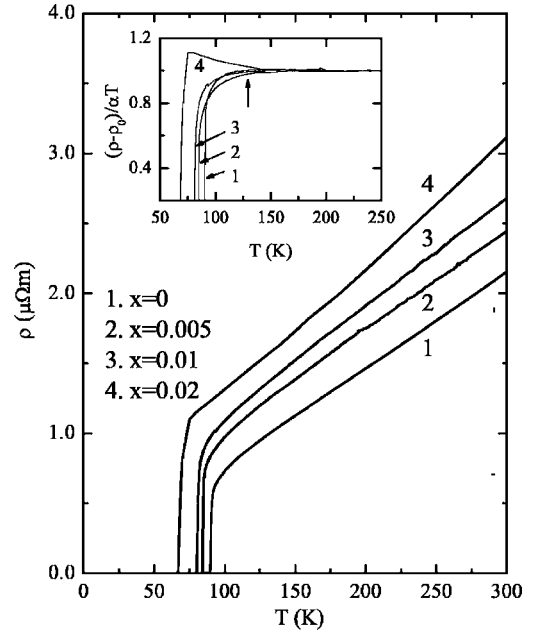


FIG. 1. The temperature dependence of in-plane resistivity for Zn-doped $\text{YBa}_2(\text{Cu}_{1-x}\text{Zn}_x)_3\text{O}_{7-\delta}$ ($x=0, 0.005, 0.01, 0.02$) thin films. The inset of Fig. 1 shows the plot of $[\rho - \rho(0)]/\alpha T$, versus temperature, where $\rho(0)$ is the $T=0$ intercept of the extrapolated *T*-linear high-temperature curve and α the slope of the linear part of the resistivity.

0.005, 0.01, 0.02) thin films. The resistivity shows linear temperature dependence at high temperature for all four samples, and it deviates downward for $x \leq 0.01$ when T approaches T_c . For the sample with $x=0.02$, the resistivity shows a small upturn at low temperature before it drops to zero at T_{c0} . Such a low-temperature upturn in ρ is usually ascribed to the localization effects. The zero-point superconducting transition temperature T_{c0} is $90, 84, 79,$ and 67 K for $x=0, 0.005, 0.01,$ and 0.02 determined from the resistive transitions, consistent with the results in literatures. The crossover temperature T^* at which $\rho(T)$ deviates downwards from linear behavior corresponds to the onset of the pseudogap opening.²⁶ To show T^* clearly, the inset of Fig. 1 shows the plot of $[\rho - \rho(0)]/\alpha T$, versus temperature, where $\rho(0)$ is the $T=0$ intercept of the extrapolated *T*-linear high-temperature curve and α the slope of the linear part of the resistivity. Due to the localization effect for $x=0.02$, T^* can not be determined reliably from the resistivity measurement. Contrast to underdoped YBCO whose T^* increases as T_c decreases with oxygen depletion, T^* is nearly unaffected by Zn doping although T_{c0} drops drastically. The insensitivity of T^* to Zn impurities has been well documented in the literatures^{27,28} for both fully oxygenated and oxygen depleted YBCO. However, it should be noted that the deviation of $\rho(T)$ below T^* becomes smaller as x increases, which means that the pseudogap is filled up by Zn doping.

The temperature dependence of Hall coefficient R_H was also measured for Zn-doped $\text{YBa}_2(\text{Cu}_{1-x}\text{Zn}_x)_3\text{O}_{7-\delta}$ ($x=0, 0.005, 0.01, 0.02$) thin films. The Hall coefficient in normal state increases slightly and the temperature dependence of R_H becomes a little weaker as Zn content increases. Accord-

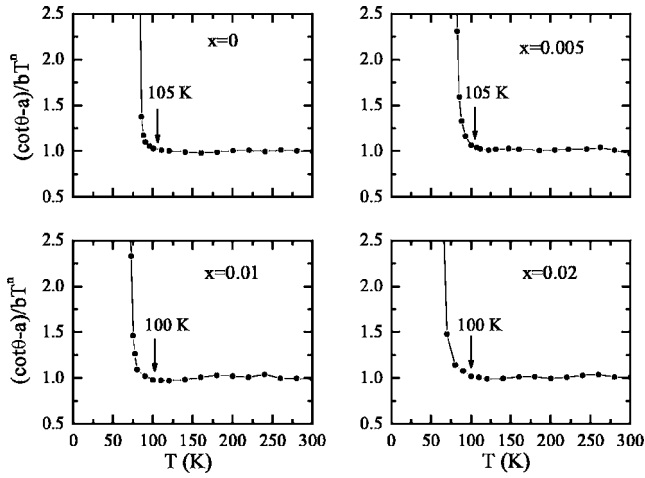


FIG. 2. The plots of $(\cot \theta - a)/bT^n$ versus T , to show the deviation from the high-temperature behavior $\cot \theta = a + bT^n$. The deviation at T_1 is marked by arrows.

ing to the previous studies,^{27,29–31} although Zn doping leads to an enhancement of the in-plane scattering rate, but the hole carrier concentration and the profile of $R_H(T)$ curves change little if the Zn content is low enough. Generally the Hall angle in the normal state satisfies the relation $\cot \theta = a + bT^2$ which can be interpreted in the two relaxation times picture.^{31,32} The peak in R_H around 100 K has been attributed to the change in the T^2 dependence of $\cot \theta$. Many studies have suggested that the peak in R_H or the change of $\cot(\theta) \times (T)$ is also associated with the opening of the pseudogap,^{26,33–36} but T_1 usually falls between T_c and T^* [determined from $\rho(T)$]. For our Zn-doped YBCO samples, $\cot \theta$ in normal state can be fitted by the function $a + bT^n$ with n close to 2. In Fig. 2 the temperature dependence of $(\cot \theta - a)/bT^n$ is shown for the four samples. The fitting parameters are $a = -61.56, 86.27, 217.65, 292.90$, $b = 0.1055, 0.0769, 0.146, 0.125$, and $n = 1.85, 1.89, 1.75, 1.76$, for $x = 0, 0.005, 0.01, 0.02$, respectively. Way above T_c , $(\cot \theta - a)/bT^n$ is quite a constant of 1 over a wide temperature range. The temperature at which $(\cot \theta - a)/bT^n$ deviates from 1 is shown by an arrow for each Zn-doping case. We define this temperature scale as T_1 . Although T_1 (~ 100 K) is lower than T^* , both are almost independent on the Zn content. However, since T_1 is always much lower than T^* , it is suggested that T_1 defines a new crossover temperature which is not related to pseudogap,³⁶ or there are two temperature scales for the pseudogap.²⁸ Matthey *et al.*³⁶ proposed that this temperature scale T_1 may be related to the superconducting fluctuation or vortexlike excitation above T_c detected by a Nernst effect measurement, which will be shown and discussed below.

The Nernst effect of all the Zn doped YBCO was measured. Figure 3 shows the traces of the Nernst signal e_y versus the applied magnetic field H of a typical sample with $x = 0.01$ ($T_{c0} = 79$ K) taken at fixed temperatures. At temperatures well below T_{c0} , all the curves have the characteristic features of the vortex Nernst effect: the signal e_y remains zero in the vortex lattice state where all the vortices are pinned; after a first order vortex solid to liquid phase transi-

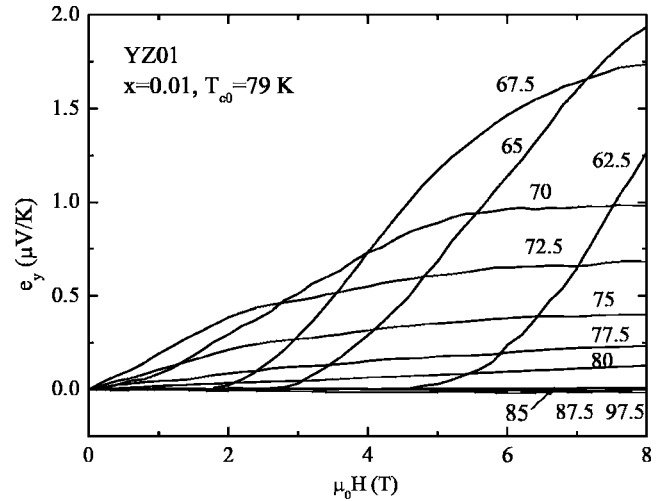


FIG. 3. The field dependence of the Nernst signal in Zn doped YBCO (sample YZ01, $x=0.01$) at fixed T from 62.5 to 97.5 K. For T just below T_{c0} ($=79$ K), $H_m \approx 0$, and e_y vs H shows a very pronounced negative curvature. H_m increases as T decreases.

tion at H_m , the motion of a large number of vortices leads to a sharp increase of e_y ; it tends to reach a maximum at a higher characteristic field scale H^* (H^* is beyond the maximum of the applied magnetic field in some low temperatures). With increasing temperatures, H_m tends to smaller values and disappears as T is close to T_{c0} . As T is above T_{c0} , the Nernst signal is still a sizeable fraction of low- T values. At higher T , the signal decreases gradually, approaching a straight line of negative slope, which we identify with the background signal ν_n from the normal charge carriers (holes). All the samples studied exhibit similar traces of e_y versus H . The temperature dependence of Nernst coefficient ν is shown for the samples with $x = 0, 0.005, 0.01$, and 0.02 in Fig. 4. The inset shows the absolute value of ν versus T in semilogarithmic scale. The arrows indicate the

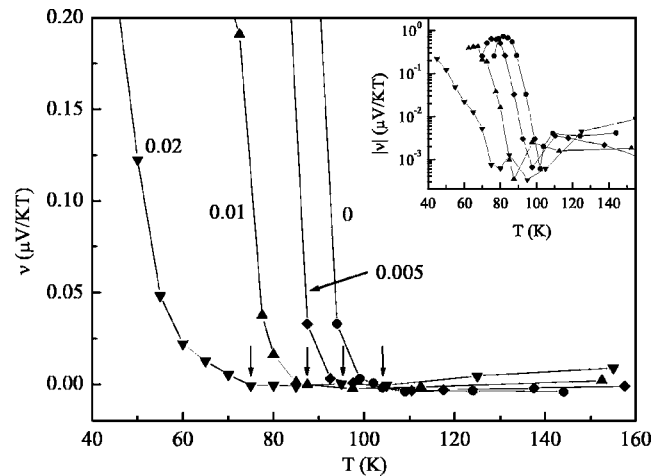


FIG. 4. The temperature dependence of ν for Zn-doped $\text{YBa}_2(\text{Cu}_{1-x}\text{Zn}_x)_3\text{O}_{7-\delta}$ ($x = 0, 0.005, 0.01, 0.02$) thin films. The temperature at which the Nernst coefficient deviates from normal state background is shown by an arrow for each case. The inset shows the semilogarithmic plot of $|\nu|$ vs T .

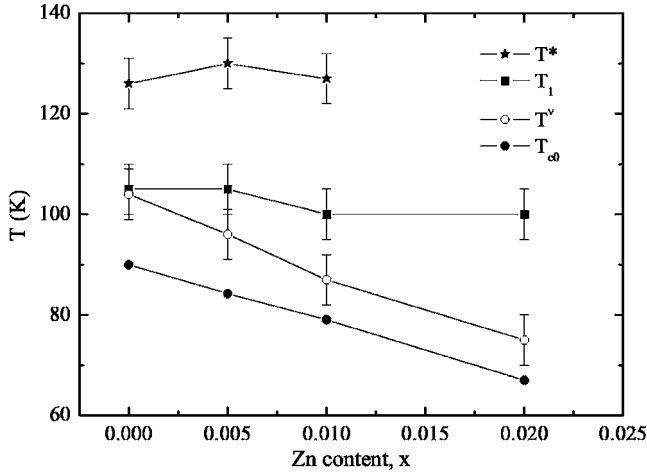


FIG. 5. The variation of T^* , T_1 , T^v , and T_{c0} with Zn content x .

onset temperature T^v at which the anomalous Nernst signal is resolved from the high-temperature normal state background ν_n . The Nernst signal in normal state is small and almost temperature independent, similar to the underdoped HTS. The contribution of normal charge carriers to the Nernst signal is usually very small in cuprates due to so-called ‘‘Sondheimer cancellation.’’³⁷ It should be mentioned that the contribution of the Cu-O chains to Nernst signal cannot be isolated in our measurement because of the twinned samples. However, we think that the intrinsic Nernst coefficient of ab plane should still be obtained because the Nernst coefficient in normal state is mainly related to the off-diagonal components of electric conductivity tensor and Peltier conductivity tensor and Ando’s group has recently confirmed that the Onsager’s reciprocal relation of resistivity [$\rho_{yx}(H) = \rho_{xy}(-H)$] still holds for YBCO regardless of the conduction of the Cu-O chains.³⁸ With decreasing temperatures, ν deviates from the high-temperature background and increases quickly at the onset temperature T^v then reaches a maximum below T_c , and finally decreases due to flux pinning. In the temperature range between T_{c0} and T^v there exists anomalously large Nernst signal, which has been interpreted as evidence for vortexlike excitations or strong superconducting fluctuations in this region. Usually T^v is lower than T^* in underdoped HTS, but it scales with T^* . However, in Zn-doped YBCO, T^v decreases quickly with x as T_{c0} does. We show the variation of T^* , T_1 , T^v , and T_{c0} with Zn content x in Fig. 5. It can be seen that while T_1 and T^* change little, T^v decreases sharply as T_{c0} does, and the interval between T_c and T^v remains almost unchanged as x increases.

It should be noted that the Nernst signal below T^v decreases as Zn content increases. The maximum of ν decreases monotonously with x while the high-temperature background of ν does not change significantly. This result is content with the conclusion that there is a drastic effect of Zn doping on the superfluid density n_s probed by μ SR measurements.¹² NMR (Refs. 3 and 4) and neutron study¹⁰ have found that Zn doping induces a localized magnetic moment in the CuO₂ plane although Zn is itself a nonmagnetic impurity. Furthermore, it has been found that the superfluid

density detected by μ SR probe decreases with Zn content and a ‘‘Swiss cheese’’ model in which charge carriers within an area $\pi\xi_{ab}^2$ around each Zn impurity are excluded from the superfluid has been proposed.¹² Recent results of a scanning tunneling microscope (STM) measurement³⁹ have also revealed that superconductivity is locally destroyed around Zn sites. Such a spatial variation of order parameter is not expected in the conventional homogeneous picture. Roughly speaking, the Nernst signal e_y is determined by the product of vortex density n_ϕ and moving velocity v_ϕ of vortex. The decrease of superfluid density leads to a decrease of n_ϕ , and the strong suppression of order parameter within a given area around Zn impurities obstructs the moving vortices like disorder potential. Therefore the sharp decrease in the maximum of Nernst signal with Zn content is consistent with the ‘‘Swiss cheese’’ model.

In underdoped La_{2-x}Sr_xCuO₄, T^v is about half of T^* and the interval between T^v and T_{c0} is as large as 100 K for $x = 0.10$.¹⁷ Such a large regime of superconducting fluctuations cannot be understood in conventional superconducting fluctuation theory. This result has been regarded as the evidence supporting the precursor superconductivity scenario to explain the pseudogap phenomena.¹⁷⁻¹⁹ However, in Zn-doped YBCO, the four temperature scales T^* , T_1 , T^v , and T_{c0} , can be divided into two categories according to their dependence on Zn content. T^* and T_1 are in one category: both are almost independent on x . In the other hand, T^v and T_{c0} are in the other category: both decrease quickly with x . T^v and T^* seems to be unrelated, which is opposite to the precursor superconductivity scenario. Namely, the anomalous Nernst signal above T_{c0} may not be related to the pseudogap. We suggest two possibilities to explain the contradictory behavior of T^v and T^* . One possibility is that preformed Cooper pairs in the pseudogap region do not exist, and T^* is the onset temperature of the fluctuations of some other types, such as antiferromagnetic fluctuations, charge density waves, or electronic phase separation (e.g., the stripe scenario), which compete or coexist with superconductivity.^{40,41} In this case Zn impurities only suppress the superconductivity and leave the fluctuation of other type unchanged. T^v which is just the onset of the superconducting fluctuation decreases with Zn content as T_{c0} does. However, the scale of T^v with T^* and the large interval between T^v and T_{c0} in underdoped cuprates are difficult to be understood in this picture. The other possibility is that T^* is the onset of precursor superconductivity which does not destroyed by Zn impurities, while the sharp decrease in the superfluid density and the spatial variation of order parameter due to Zn doping makes the vortexlike excitations above T_{c0} weak and undetectable by Nernst effect measurement, leading to a decrease of T^v . The fact that the sharp decrease in the maximum of Nernst signal with Zn content below T_{c0} also supports this picture. We suggest that Zn doping does not have much influence on the pseudogap opening, and therefore neither T_1 nor T^* changes much with Zn content. However, Zn impurities cause a notable decrease in the superfluid density, and therefore suppress both T^v and T_{c0} .

IV. CONCLUSION

In conclusion, we have studied the transport properties, including resistivity, Hall effect and Nernst effect in a series

of Zn-doped $\text{YBa}_2(\text{Cu}_{1-x}\text{Zn}_x)_3\text{O}_{7-\delta}$ epitaxial thin films. It is found that the pseudogap temperature T^* determined from the temperature dependence of resistivity and the temperature scale T_1 determined from the T^n dependence of $\cot \theta$ remain unchanged, meanwhile the onset temperature T^v of vortexlike excitation above T_{c0} determined from Nernst effect drops sharply with increasing Zn content as the superconducting critical temperature T_{c0} does. We also find that the vortex Nernst signal in mixed state decreases quickly with increasing x . The variations of T^* and T^v with x might be understood in the picture that Zn doping does not destroy the precursor superconductivity, but causes a sharp decrease

in the superfluid density and spatial variation of the order parameter, as suggested in the “Swiss cheese” model.

ACKNOWLEDGMENTS

The authors would like to thank C. M. Feng for help on transport measurements and thank G. H. Cao for fruitful discussions. This work was supported by the National Natural Science Foundation of China (Grant No. 10225417) and the Ministry of Science and Technology of China (Project No. NKBRSF-G1999064602).

*Electronic address: zhuan@css.zju.edu.cn

- ¹Y. Sun and K. Maki, *Phys. Rev. B* **51**, 6059 (1995).
- ²R. J. Radtke, K. Levin, H.-B. Schuttler, and M. R. Norman, *Phys. Rev. B* **48**, 653 (1993).
- ³H. Alloul, P. Mendels, H. Casalta, J. F. Marucco, and J. Arabshi, *Phys. Rev. Lett.* **67**, 3140 (1991).
- ⁴M.-H. Julien, T. Feher, M. Horvatic, C. Berthier, O. N. Bakharev, P. Segransan, G. Collin, and J.-F. Marucco, *Phys. Rev. Lett.* **84**, 3422 (2000).
- ⁵Y. Fukuzumi, K. Mizuhashi, K. Takenaka, and S. Uchida, *Phys. Rev. Lett.* **76**, 684 (1996).
- ⁶C. Panagopoulos, J. R. Cooper, N. Athanassopoulou, and J. Chrosch, *Phys. Rev. B* **54**, R12721 (1996).
- ⁷J. W. Loram, K. A. Mirza, J. M. Wade, J. R. Cooper, and W. Y. Liang, *Physica C* **235-240**, 134 (1994).
- ⁸D. N. Basov, B. Dabrowski, and T. Timusk, *Phys. Rev. Lett.* **81**, 2132 (1998).
- ⁹N. L. Wang, S. Tajima, A. I. Rykov, and K. Tomimoto, *Phys. Rev. B* **57**, R11081 (1998).
- ¹⁰K. Kakurai, S. Shamoto, T. Kiyokura, M. Sato, J. M. Tranquada, and G. Shirane, *Phys. Rev. B* **48**, 3485 (1993).
- ¹¹C. Bernhard, J. L. Tallon, C. Bucci, R. De Renzi, G. Guidi, G. V. M. Williams, and Ch. Niedermayer, *Phys. Rev. Lett.* **77**, 2304 (1996).
- ¹²B. Nachumi, A. Keren, K. Kojima, M. Larkin, G. M. Luke, J. Merrin, O. Tchernyshöv, Y. J. Uemura, N. Ichikawa, M. Goto, and S. Uchida, *Phys. Rev. Lett.* **77**, 5421 (1996).
- ¹³E. Altendorf, J. C. Irwin, W. N. Hardy, and R. Liang, *Physica C* **185-189**, 1375 (1991).
- ¹⁴A. Matic, M. Kall, L. Borjesson, and Y. Eltsev, *J. Phys. Chem. Solids* **56**, 1835 (1995).
- ¹⁵M. F. Limonov, A. I. Rykov, S. Tajima, and A. Yamanaka, *Phys. Rev. B* **61**, 12412 (2000).
- ¹⁶M. Limonov, D. Shantsev, S. Tajima, and A. Yamanaka, *Physica C* **357-360**, 265 (2001).
- ¹⁷Z. A. Xu, N. P. Ong, Y. Wang, T. Kakeshita, and S. Uchida, *Nature (London)* **406**, 486 (2000).
- ¹⁸Y. Wang, N. P. Ong, Z. A. Xu, T. Kakeshita, S. Uchida, D. A. Bonn, R. Liang, and W. N. Hardy, *Phys. Rev. Lett.* **88**, 257003 (2002).
- ¹⁹Y. Wang, S. Ono, Y. Onose, G. Gu, Y. Ando, Y. Tokura, S. Uchida, and N. P. Ong, *Science* **299**, 86 (2003).
- ²⁰V. J. Emery and S. A. Kivelson, *Nature (London)* **374**, 434 (1995).
- ²¹H. Kontani, *Phys. Rev. Lett.* **89**, 237003 (2002).
- ²²I. Ussishkin, S. L. Sondhi, and D. A. Huse, *Phys. Rev. Lett.* **89**, 287001 (2002).
- ²³C. Timm, D. Manske, and K. H. Bennemann, *Phys. Rev. B* **66**, 094515 (2002).
- ²⁴E. W. Carlson, V. J. Emery, S. A. Kivelson, and D. Orgad, *cond-mat/0206217* (unpublished).
- ²⁵Z. Y. Weng and V. N. Muthukumar, *Phys. Rev. B* **66**, 094509 (2002).
- ²⁶T. Ito, K. Takenaka, and S. Uchida, *Phys. Rev. Lett.* **70**, 3995 (1993).
- ²⁷D. J. C. Walker, A. P. Mackenzie, and J. R. Cooper, *Phys. Rev. B* **51**, 15653 (1995).
- ²⁸Y. Abe, K. Segawa, and Y. Ando, *Phys. Rev. B* **60**, R15055 (1999).
- ²⁹G. Xiao, M. Z. Cieplak, A. Gavrin, F. H. Streitz, A. Bakhshai, and C. L. Chien, *Phys. Rev. Lett.* **60**, 1446 (1988).
- ³⁰J. R. Cooper, S. D. Obertelli, P. A. Freeman, D. N. Zheng, J. W. Loram, and W. Y. Liang, *Semicond. Sci. Technol.* **4**, S277 (1991).
- ³¹T. R. Chien, Z. Z. Wang, and N. P. Ong, *Phys. Rev. Lett.* **67**, 2088 (1991).
- ³²P. W. Anderson, *Phys. Rev. Lett.* **67**, 2092 (1991).
- ³³B. Bucher, P. Steiner, J. Karpinski, E. Kaldis, and P. Wachter, *Phys. Rev. Lett.* **70**, 2012 (1993).
- ³⁴H. Y. Hwang, B. Batlogg, H. Takagi, H. L. Kao, J. Kwo, R. J. Cava, J. J. Krajewski, and W. F. Peck, Jr., *Phys. Rev. Lett.* **72**, 2636 (1994).
- ³⁵R. Jin and H. R. Ott, *Phys. Rev. B* **57**, 13872 (1998).
- ³⁶D. Matthey, S. Gariglio, B. Giovannini, and J.-M. Triscone, *Phys. Rev. B* **64**, 024513 (2001).
- ³⁷E. H. Sondheimer, *Proc. R. Soc. London, Ser. A* **193**, 484 (1948).
- ³⁸K. Segawa and Y. Ando, *Phys. Rev. B* **69**, 104521 (2004).
- ³⁹S. H. Pan, E. W. Hudson, K. M. Lang, H. Eisaki, S. Uchida, and J. C. Davis, *Nature (London)* **403**, 746 (2000).
- ⁴⁰J. L. Tallon, G. V. M. Williams, M. P. Staines, and C. Bernhard, *Physica C* **235-240**, 1821 (1994).
- ⁴¹J. L. Tallon and J. W. Loram, *Physica C* **349**, 53 (2001).